D 5.1 Detailed theoretical schemes for the realization of modular entagnglement and universal quantum integration

Entanglement Amplification in the Non-Perturbative Dynamics of Modular Quantum Systems

A. Bayat[1], S. M. Giampaolo[2], F. Illuminati[2], and M. B. Plenio[1]

[1] *Institut für Theoretische Physik, Albert-Einstein-Allee 11, Universität Ulm, D-89069 Ulm, Germany*
[2] *Dipartimento di Ingegneria Industriale, Università degli Studi di Salerno, Via Ponte don Melillo, I-84084 Fisciano (SA), Italy*

(Dated: March 12, 2013)

We analyze the conditions for entanglement amplification between distant and not directly interacting quantum objects by their common coupling to media with static modular structure and subject to a local (single-bond) quenched dynamics. We show that in the non-perturbative regime of the dynamics the initial end-to-end entanglement is strongly amplified and, moreover, can be distributed efficiently between distant objects. Due to its intrinsic local and non-perturbative nature the dynamics is fast and robust against thermal fluctuations, and its control is undemanding. We show that the origin of entanglement amplification lies in the interference of the ground state and at most one of the low-lying energy eigenstates. The scheme can be generalized to provide a fast and efficient router for generating entanglement between simultaneous multiple users.

PACS numbers: 03.67.-a, 03.67.Hk, 03.65.Ud, 75.10.Pq, 75.20.Hr

Realizing a sizable and stable entanglement between distant qubits is a crucial stage in performing fundamental tasks of quantum information and communication [1]. In the ground state of noncritical strongly correlated systems with short-range interactions the 2-points correlation functions and thus the entanglement between spins can be proven to vanish exponentially with the distance [2]. To overcome this problem, a possibility is to mediate indirect interactions between distant qubits by a suitable quantum many-body medium. For instance, one can exploit impurities weakly coupled to the ends of a spin chain that mediates an indirect interaction and creates a strong long-distance entanglement between them [3]. Indeed, it has been shown that a relatively large family of strongly correlated many-body systems allows for this possibility [4–6]. However, for most of these systems the energy gap is exponentially decreasing in the size of the system, so that even for short chains the mechanism becomes thermally unstable: very small thermal fluctuations are sufficient to mix the ground state with higher energy eigenstates and suppress the entanglement between the end impurities. One can introduce systems with interaction patterns such that the gap closes algebraically with the distance [4]; in this case the thermal stability improves at the price of letting the end-to-end entanglement become weakly decreasing with the size of the system [4, 5]. Even if all these results can be extended to higher dimensional systems [7] this appears to be the unavoidable limit of a a purely static, ground-state approach [8]

On the other hand, it is well known that properly tailored time evolutions can propagate entanglement through many-body systems [9]. In particular, global [10] or local quantum quenches [11–14] can create long-distance entanglement. Apart from certain perturbative proposals that suffer from a very slow convergence [11–13], the dynamical schemes in general do not require the weak end coupling assumption [9, 10, 14, 15] and hence thermal instability is not as dramatic issue as in the case of static schemes. Rather, the price to be payed is the need for a very accurate tuning of the times at which optimal entanglement is generated and thus a much more elaborate control on the system. In conclusion, entangling distant qubits can be realized either via static or dynamic approaches, however, either at the price of a strong thermal instability or an excessively demanding control.

In the present work we introduce a scheme that combines the modular-static and the quench-dynamic approaches to entanglement generation and distribution among distant qubits. The proposed mixed scheme strongly reduces the drawbacks of both approaches and realizes a novel mechanism of entanglement amplification starting from weakly entangled inputs. In our model, a quantum spin chain is split into two elementary bulk modules. Two end impurities are attached to each module with couplings of arbitrary strength. This initial static configuration is then evolved through a sudden quench of the bond connecting the two modules. We show that the generated end-to-end entanglement across the entire system is always larger than the initial entanglement at the ends of each module and that this *entanglement amplification* can always be achieved for all parameter ranges. As the length of each module is half the total size of the system and the impurity couplings are non perturbative, the energy gap remains sizable even for very long chains and stability against thermal fluctuations is assured even at moderately high temperatures. Moreover, by exploiting just a single bond quench for inducing a nontrivial dynamics, the required control is minimal. This mechanism can demonstrate an entanglement router which unlike previous proposals neither needs AC-control of the couplings [16] nor the presence of both ferromagnetic and anti-ferromagnetic couplings simultaneously [17]. Furthermore, the entanglement amplification mechanism finds a clear physical explanation in the quantum interference between only two eigenvectors (ground and one of the low-lying excited energy eigenstates) of the final Hamiltonian.

The model. We consider two independent one-dimensional arrays of qubits, the *modules*. Each module is constituted by a bulk of spins coupled at both ends with two impurities. The interaction Hamiltonian for each module reads:

$$H_k \;=\; J_k' J(h^{(k)}_{1,2} + h^{(k)}_{N_k-1,N_k}) + J\sum_{i=2}^{N_k-2} h^{(k)}_{i,i+1}\;,$$

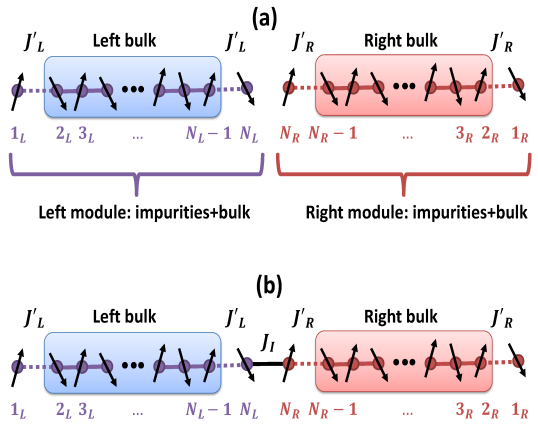

FIG. 1: (Color online) (a) A schematic picture of two independent modules and their couplings to the respective end impurities. (b) Onset of a quenched interaction dynamics between the two modules by switching on instantaneously a strong bond J_I between the impurities at the module-module boundary.

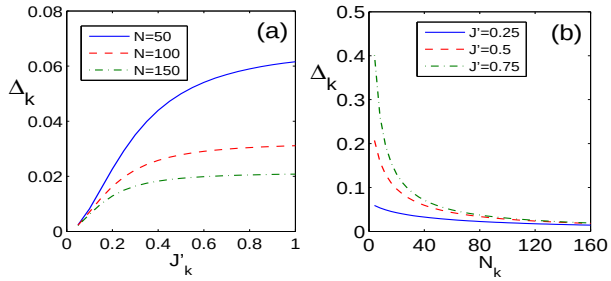

FIG. 2: (Color online) Energy gap Δ_k of a single XX module as a function of: (a) the coupling J' to the end impurities for different sizes N_k of the module; (b) the size N_k for different values of J'.

$$h_{i,j}^{(k)} = X_i^{(k)}X_j^{(k)} + Y_i^{(k)}Y_j^{(k)} + \delta Z_i^{(k)}Z_j^{(k)} , \qquad (1)$$

where $k = L, R$ denotes the left or right module, respectively with $N_k = N_L, N_R$ spins, $\{X_i^{(k)}, Y_i^{(k)}, Z_i^{(k)}\}$ are the Pauli spin operators at site i in the k-th module, $J > 0$ is the exchange spin-spin coupling strength, $J'_k > 0$ specifies the coupling to the end impurities, and δ is the interaction anisotropy along the z direction. A schematic picture of this system is shown in Fig. 1 (a) (note the mirror inversion of spin numbering in each module). The spin-$1/2$ XXZ Hamiltonian Eq. (1) for each module has a rich zero-temperature quantum phase diagram; in particular, for $-1 \leq \delta \leq 1$, the system is in the so-called gapless XY antiferromagnetic phase that admits a nondegenerate, highly entangled ground state. In the two fully isotropic limits one recovers the relevant cases of the XX Hamiltonian ($\delta = 0$) and the Heisenberg (XXX) Hamiltonian ($\delta = 1$).

Static end-to-end entanglement in modules. Let us first discuss the entanglement between the two end impurities in the ground state of a single module. The model in Eq. (1) exhibits long-distance entanglement in the ground state when the module has *even* length N_k and $J'_k < J$ so that the spins in the bulk tend to entangle between themselves and consequently the two end impurities are forced to get entangled [4, 5]. From the ground state of the XXZ Hamiltonian H_k, one can compute the initial reduced density matrix of the two impurities by tracing out the spins of the bulk. Due to the symmetries of the system, the reduced state is diagonal in the Bell basis

$$\rho_{1_k,N_k} = P_k^s |\psi^-\rangle\langle\psi^-| + \sum_{\alpha=x,y,z} P_k^\alpha |B^\alpha\rangle\langle B^\alpha|, \qquad (2)$$

where $|\psi^-\rangle$ is the singlet state, P_k^s is the singlet fraction, $|B^\alpha\rangle$ (for $\alpha = x, y, z$) are the other Bell states which can be obtained by applying the α Pauli operator on one part of the singlet, and the P_k^α's account for their contributions. For a fixed length N_k, one can increase P_k^s arbitrarily and create large entanglement between the two impurities by decreasing J'_k. However, by decreasing J'_k the energy gap of the system also decreases, at best algebraically [4, 5]; when the thermal energy $k_B T$ becomes comparable with the gap, the state of the system becomes a mixed thermal state with no entanglement between the end impurities. In Fig. 2(a) the energy gap Δ is plotted as a function of J'_k for a XX module of length N_k which clearly shows an exponential decay for small J'_k's. Of course, the gap also decays with the size N_k as shown in Fig. 2(b).

Dynamical entanglement generation in a modular quantum spin chain. Given the initial static situation with the two modules in their respective ground states, we introduce a quench dynamics between them. The two even-sized modules of lengths N_L and N_R are described via the Hamiltonians H_L and H_R introduced in Eq. (1). The exchange coupling J and anisotropic parameter δ are assumed to be identical in both modules, while the couplings with the end impurities are respectively J'_L and J'_R. The initial ground state of a chain of total lengt $N = N_L + N_R$ formed by the two noninteracting modules is obviously the tensor product of the ground states of the two subsystems: $|\psi(0)\rangle = |GS_L\rangle \otimes |GS_R\rangle$. At $t = 0$ one switches on the interaction between the two modules:

$$H_I = J_I (X_{N_L}^{(L)} X_{N_R}^{(R)} + Y_{N_L}^{(L)} Y_{N_R}^{(R)} + \delta Z_{N_L}^{(L)} Z_{N_R}^{(R)}) , \qquad (3)$$

where J_I is the bond that couples the two modules. The total Hamiltonian of the system at $t > 0$ becomes, as schematicly represented in Fig. 1(b), $H_T = H_L + H_R + H_I$. The initial product state is not an eigenvector of H_T and the system evolves according to $|\psi(t)\rangle = e^{-iH_T t}|\psi(0)\rangle$. The reduced state of the two end impurities at time t is

$$\rho_{1_L,1_R}(t) = P_{out}^s(t) |\psi^-\rangle\langle\psi^-| + \sum_{\alpha=x,y,z} P_{out}^\alpha(t) |B^\alpha\rangle\langle B^\alpha|.$$

We use relative entropy of entanglement [18] as an operational measure to quantify the entanglement content of the two ending impurities at sites 1_L and 1_R defined by

$$E_{1_L,1_R}(t) = 1 - H\left(P_{out}^s(t)\right) \qquad (4)$$

where $H(x)=-x\log_2 x-(1-x)\log_2(1-x)$. This is of course related to the concurrence [19] of the two impurities $C_{1_L,1_R}(t)$ via $E_{1_L,1_R}(t)=1-H\left((C_{1_L,1_R}(t)+1)/2\right)$ and always give a lower value with respect to concurrence.

Perturbative regime. We first study the case of J'_L and J'_R both sufficiently small so that the pairs of end impurities in each module are initially highly entangled (strong initial end-to-end entanglement in both modules). In this situation, in each module the impurities are effectively decoupled from the rest of the system and resorting to the Schrieffer-Wolff transformation [20] one obtains an effective interaction Hamiltonian for the impurities in each module

$$H^k_{eff}=J^k_{eff}(X^k_{1_k}X^k_{N_k}+Y^k_{1_k}Y^k_{N_k}+\delta Z^k_{1_k}Z^k_{N_k})\ , \quad (5)$$

where the effective coupling is linear in the energy gap: $J^k_{eff}=\Delta_k/4$ with $k=L,R$. Fixing the inter-module interaction bond at $J_I=J^L_{eff}+J^R_{eff}$, as shown in Fig. 1(b), one has that $E_{1_L,1_R}(t)=1-H\left(\frac{5-3\cos(4J_It)}{8}\right)$. Therefore, at the optimal time $t_{opt}=\frac{\pi}{4J_I}$, the maximal long-distance entanglement is established between the ending sites. Compared to the static case with a single long module of length N with the same entanglement between the end impurities 1_L and 1_R, the dynamical mechanism in the perturbative regime assures a larger thermal stability "per sé". If the entangling time t_{opt} is engineered so to be much smaller than the thermalization time, then the thermal effects are fully determined by the thermal initial state associated to the energy gap of each module, which is always above and can be made much larger than the gap of the two combined in a single one of size $N=N_L+N_R$. In the dynamic case one can exploit larger impurity couplings J'_k for each module in comparison to the static case with a single module of size N, thus increasing the gap, as illustrated in Fig. 2(a). In this way thermal instability is ameliorated but not fixed; moreover, the perturbative nature of the coupling J_I implies a very slow dynamics. The power of the scheme shows only in the non-perturbative regime.

Non-perturbative regime: Entanglement amplification. When the strength of the coupling to the impurities becomes comparable to the interaction energies in the bulk, the initial end-to-end entanglement for each module is strongly suppressed, the reduction to the effective Hamiltonians Eq. (5) is no longer justified, and J_I cannot be determined analytically as in the perturbative regime. To proceed, one can observe that in practice the affordable time for the entangling dynamics is ultimately bounded by the decoherence rates. Introducing such upper bounds for the optimal entangling time, we define an optimization problem for the largest attainable end-to-end entanglement that depends on two free parameters, i.e. the static coupling to the end impurities $J'=J'_L=J'_R$ and the quench-dynamic bond J_I between the two modules. In Fig. 3(a) the end-to-end entanglement $E_{1_L,1_R}(t)$ is plotted as a function of time both for the Heisenberg and the XX Hamiltonians for different values of J' and J_I. As reported in Fig. 3(a), the time evolution after the quench generates a large end-to-end entanglement, strongly amplified respect

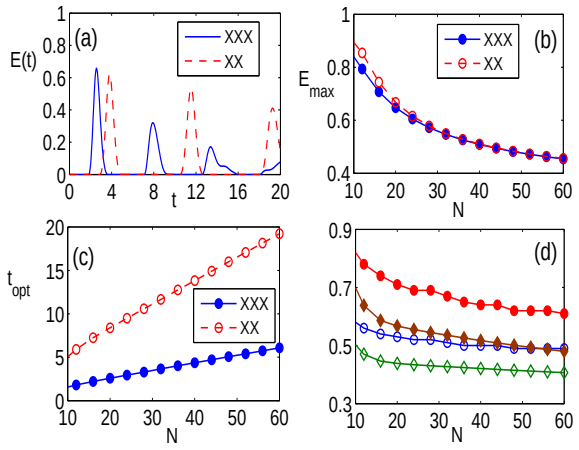

FIG. 3: (Color online) (a) End-to-end entanglement as a function of time for N_L=N_R=10, J'=0.5 and J_I=0.65. (b) E_{max} as a function of N. (c) Optimal time t_{opt} versus length N. (d) Optimal impurity coupling J'_{opt} for XXX (open blue circles) and XX (green open diamonds) and optimal interaction coupling J_I^{opt} for XXX (filled red circles) and XX (filled brown diamonds).

to the initial one in each module. The optimal entangling time t_{opt} is then the earliest time at which the end-to-end entanglement peaks, defining its maximum attainable value: $E_{max}=E(t_{opt})$. In Fig. 3(b) we plot E_{max} as a function of the total chain's size N when both J' and J_I are tuned to their optimal values. One has that for long enough chains both the XX and Heisenberg Hamiltonians perform equally well. However, if we look at Fig. 3(c), where t_{opt} is reported as a function of N, one can see that the Heisenberg chain generates a faster dynamics with earlier peaks, an important added value in order to minimize the effects of decoherence. Finally, in Fig. 3(d) we report the optimal values J'_{opt} and J_I^{opt}, respectively of the coupling to the end impurities and the interaction coupling in the bulk, as functions of N. Remarkably, as Fig. 3(d) clearly shows, one finds that the optimal couplings decrease very slowly by increasing the size N, implying the onset of a fast dynamics and the permanence of the non-perturbative regime even for very long chains. Furthermore, larger couplings in Heisenberg chains in compare to XX ones results in a faster dynamics and provides higher energy gap and thus higher thermal stability.

To show how entanglement is actually amplified by the dynamical process we compare the initial static end-to-end entanglement $E_{1_L,N_L}(0)$ in the ground state of a single module of length $N_L=N/2$ and the output dynamical end-to-end entanglement $E_{1_L,1_R}(t_{opt})$ at the optimal entangling time across two interacting modules forming a chain of total length N_L+$N_R=N$. Fig. 4(a) shows that the initial ground-state end-to-end entanglement is *always* amplified for the entire range of couplings J' to the end impurities. A remarkable rebound of $E_{1_L,1_R}(t_{opt})$ occurs at a point of non-analyticity that separates the perturbative from the non-perturbative regime, corresponding to the onset of enhanced dynamical amplification

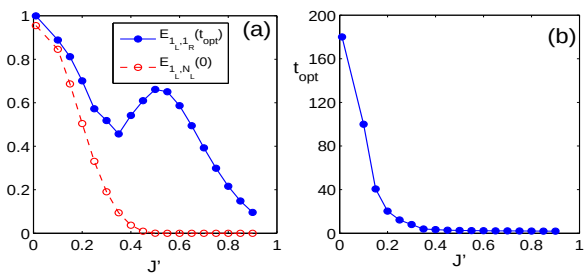

FIG. 4: (Color online) (a) The initial, static end-to-end entanglement $E_{1_{L},N_{L}}(0)$ (or $E_{1_{R},N_{R}}(0)$) in each single module of length $N_L = N_R = 10$ together with the maximal end-to-end dynamical entanglement $E_{1_{L},1_{R}}(t_{opt}$ for the entire two-module chain of length $N = N_L + N_R$, as functions of the coupling J' for $\delta = 1$. (b) The optimal time t_{opt} at which entanglement peaks, as a function of J'.

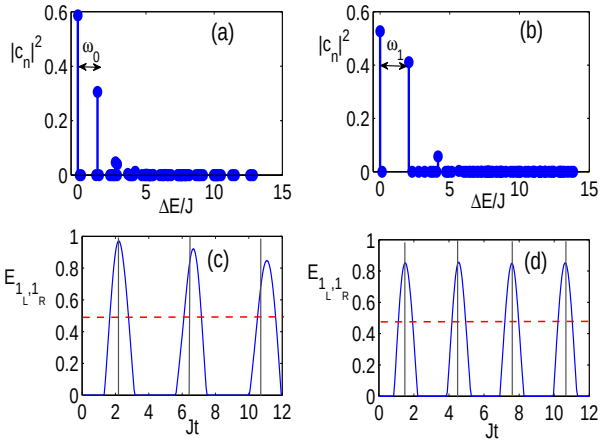

FIG. 5: (Color online) Upper panels: $|c_n^2|$ versus $\Delta E/J = (E_n - E_0)/J$ for all eigenvectors of H_T for two chains with $N_L = N_R = 4$, $J'_L = J'_R = 0.5J$, $J_I = 0.75J$ where J is the bulk amplitude for (a) $\delta = 0$; (b) $\delta = 1$. Lower panels: $E_{1_{L},1_{R}}$ vs. time for the two chains with parameters given above and (c) $\delta = 0$; (d) $\delta = 1$. The red dashed lines stand for the initial end to end entanglement in each single chain. The vertical gray lines signal the times at which the phase $\phi(t) = \exp(-i\omega_\delta t) = -1$.

against pure decay. In order to characterize and understand these two different regimes and the transition between them we have studied the entangling time t_{opt} as a function of the coupling J' to the end impurities. Fig. 4 (b) illustrates that in the perturbative regime t_{opt} increases exponentially with decreasing J', while in the non-perturbative regime it remains essentially flat at very small values, guaranteeing, for appropriately chosen values of J', that maximal amplification occurs well in advance of the effects of decoherence.

Origin of amplification: Excitation spectrum and quantum interference. To understand the physical mechanism underlying entanglement amplification in the non-perturbative dynamics of modular many-body systems we must take notice of the fact that $|\psi(t)\rangle = \sum_{n=1}^{2^N} c_n e^{-iE_n t}|E_n\rangle$, where, $E_n(|E_n\rangle)$ is the n-th eigenvalue (eigenvector) of H_T and $c_n = \langle E_n|\psi(0)\rangle$. When the values of the Hamiltonian parameters J' and J_I are far from their optimal values, many of c_n's are significantly different from zero. At values close to the optimal set the situation becomes radically different, as reported in Figs. 5(a) and (b), where the squared amplitudes $|c_n|^2$ are plotted as functions of the energy difference between the corresponding n-th eigenstate and the ground state of H_T, respectively for the XX ($\delta = 0$, Fig. 5(a)) and the Heisenberg Hamiltonian ($\delta = 1$, Fig. 5(a)). In both cases the initial state is essentially projected onto only two eigenstates of H_T, the ground state and just one of the first few low-lying excited states. Therefore the evolution of the initial state at time t under the action of H_T is essentially due to the relative phase factor $\phi(t) = \exp(-i\omega_\delta t)$, where ω_δ is the the difference of the eigenvalues of the two eigenstates as indicated in Figs. 5(a) and (b). As shown in Figs. 5(c) and(d), the maximum of the entanglement amplification is reached when $\phi(t) \simeq -1$. Therefore the dynamic amplification of long-distance entanglement is essentially due to a constructive interference between the two eigenstate while the fact that the maximum is reached around and not exactly at $\phi(t) = -1$ accounts for the projections on the remaining part of the spectrum: although strongly suppressed, they are not exactly vanishing. As we move to values of the Hamiltonian parameters away from the optimal ones and/or the dimension of the two modules is increased, the relative weight of the other eigenstates becomes more relevant reducing the maximum value reached by $E_{1_{L},1_{R}}$.

Conclusions & Outlook: Entanglement router. By considering many-body media with static structures of bulk modules and by engineering suitably quenched local interaction dynamics between different modules, we have introduced a method for the generation and amplification of entanglement between distant and non-interacting quantum objects. The method is intrinsically non-perturbative and does not require sophisticated controls of the system dynamics. Indeed, we showed that the end-to-end entanglement initially present in the ground state of a modular many-body system is amplified by the quenched dynamics whenever all the values of the Hamiltonian parameters are far from the perturbative regime. The ensuing entangling dynamics is fast and robust against thermal fluctuations. The occurrence of such dynamical mechanism of entanglement amplification finds a simple and beautiful explanation in the constructive interference of only two energy eigenstates of the driving Hamiltonian. This opens potentially many new perspective for studying entanglement generation, distribution, and manipulation across arbitrary distances in a many-body systems. Our minimal control strategy applies immediately to the demonstration of an entanglement router capable of distributing entanglement simultaneously between multiple users. Indeed, consider a setup in which every user controls one impurity in a module which extends from its position to a common dispatching center where the other impurities are controlled. In the dispatching center, one can switch on the interaction between any pair of impurities of different modules and switch on the

quenched entangling dynamics in those particular chains, thus creating entanglement directly between the two users. The main advantage of such an entanglement router is the minimal control needed (a single bond quench) that, at variance with previous router proposals, neither requires AC-control of the couplings [16] nor the introduction of many different couplings [17].

Acknowledgements: AB and MBP acknowledge financial support from the EU STREP project PICC and the Alexander von Humboldt foundation. SMG and FI acknowledge financial support from the EU STREP Project iQIT, Grant Agreement No. 270843.

[1] M. A. Nielsen and I. L. Chuang, *Quantum Computation and Quantum Information* (Cambridge University Press, Cambridge, 2000).

[2] M.B. Plenio, J. Eisert, J. Dreissig and M. Cramer, Phys. Rev. Lett. **94**, 060503 (2005); M.B. Hastings and T. Koma, Comm. Math. Phys. **265**, 781 (2006)

[3] L. Campos Venuti, C. Degli Esposti Boschi, and M. Roncaglia, Phys. Rev. Lett. **96**, 247206 (2006).

[4] L. Campos Venuti, S. M. Giampaolo, F. Illuminati, and P. Zanardi, Phys. Rev. A **76**, 052328 (2007).

[5] S. M. Giampaolo and F. Illuminati, New J. Phys. **12**, 025019 (2010); S. M. Giampaolo and F. Illuminati, Phys. Rev. A **80**, 050301 (2009).

[6] G. Gualdi, S. M. Giampaolo, and F. Illuminati, Phys. Rev. Lett. **106**, 050501 (2011).

[7] S. Zippili, S. M. Giampaolo and F. Illuminati arXiv:1302.1205.

[8] T. Kuwahara, New J. Phys. **14**, 123032 (2012).

[9] S. Bose, Contemporary Physics **48**, 13 (2007).

[10] J. Eisert, M.B. Plenio, S. Bose and J. Hartley, Phys. Rev. Lett. **93**, 190402 (2004); H. Wichterich and S. Bose, Phys. Rev. A **79**, 060302(R) (2009); K. Sengupta and D. Sen, Phys. Rev. A **80**, 032304 (2009).

[11] L. Campos Venuti, C. Degli Esposti Boschi, and M. Roncaglia, Phys. Rev. Lett. **99**, 060401 (2007).

[12] M. J. Hartmann, M. E. Reuter, and M. B. Plenio, New J. Phys. **8**, 94 (2006).

[13] Y. Li, T. Shi, B. Chen, Z. Song, and C.-P. Sun, Phys. Rev. A **71**, 022301 (2005); A. Wójcik, T. Łuczak, P. Kurzyński, A. Grudka, T. Gdala, and M. Bednarska, Phys. Rev. A **72**, 034303 (2005).

[14] A. Bayat, S. Bose, and P. Sodano, Phys. Rev. Lett. **105**, 187204 (2010).

[15] L. Banchi, A. Bayat, P. Verrucchi, and S. Bose, Phys. Rev. Lett. **106**, 140501 (2011).

[16] D. Zueco, F. Galve, S. Kohler, and P. Hänggi, Phys. Rev. A **80**, 042303 (2009); S. M. Giampaolo, F. Illuminati, A. Di Lisi, and G. Mazzarella, Int. J. Quant. Inf. **4**, 507 (2006); S. M. Giampaolo, F. Illuminati, A. Di Lisi, and S. De Siena, Laser Physics **16**, 1411 (2006).

[17] M.B. Plenio, J. Hartley and J. Eisert, New J. Phys. **6**, 36 (2004); P. J. Pemberton-Ross and A. Kay, Phys. Rev. Lett. **106**, 020503 (2011).

[18] V. Vedral, M.B. Plenio, M.A. Rippin and P.L. Knight, Phys. Rev. Lett. **78**, 2275 (1997).

[19] W.K. Wootters Phys. Rev. Lett. **80**, 2245 (1998).

[20] S. Bravyi, D. P. DiVincenzo, and D. Loss, Ann. Phys. (N.Y.) **326**, 2793 (2011).